

Electrical Vehicle Battery Charger Based On Cuk-Sepic Converter Design



Author

Hajira Nadeem

MS-20(EE)

00000326877

Supervisor

DR. SARMAJ MAJEED MALIK

DEPARTMENT OF ELECTRICAL ENGINEERING

COLLEGE OF ELECTRICAL & MECHANICAL ENGINEERING


NATIONAL UNIVERSITY OF SCIENCES AND TECHNOLOGY


ISLAMABAD

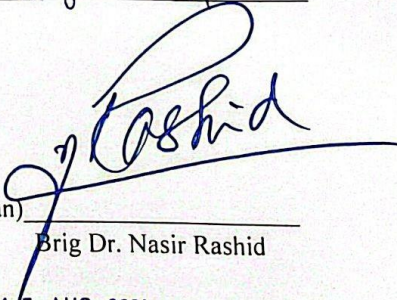
August 2024

THESIS ACCEPTANCE CERTIFICATE

It is certified that final copy of MS/MPhil thesis written by Ms. Hajira Nadeem (Registration No. 00000326877) Entry-2020, of (College of E&ME) has been vetted by the undersigned, found complete in all respects as per NUST Statutes/Regulations, is free of plagiarism, errors, and mistake and is accepted as partial fulfillment for award of MS degree. It is further certified that necessary amendments as pointed out by GEC member of the scholar have also been incorporated in the said thesis.

Signature: 
Name of Supervisor Dr. Sarmad Majeed Malik
Date: 15/8/24

Signature (HoD): 
Dr. Qasim Umar Khan
Date: 15-Aug-2024

Signature (Dean) 
Brig Dr. Nasir Rashid
Date: 15 AUG 2024

DEDICATION

This thesis is dedicated to my beloved parents and teachers. Without their unwavering support, encouragement, and efforts, this achievement would not have been possible. Their belief in me has been my greatest strength.

ACKNOWLEDGEMENT

I am deeply grateful to my Creator, Allah Almighty, for His guidance at every step of this journey. Without His invaluable help and direction, none of this would have been possible. He has empowered me with the ability to read and write and granted me the knowledge I now carry forward.

I am here to extend my heartfelt thanks to the supervisor, Dr. Sarmad Majeed Malik, for his support throughout my thesis and for the knowledge, he imparted through his courses. I am also immensely thankful to Dr. Taosif Iqbal, Dr. Usman Ali and Engr. Wahaj Ahmed Khan Afridi for their significant support and cooperation.

Hajira Nadeem

ABSTRACT

This paper introduces a groundbreaking advancement in electric vehicle technology: a sophisticated single-stage battery charger featuring an isolated bridgeless (BLS) CukSEPIC converter (CSC). Operating seamlessly in discontinuous conduction mode and seamlessly integrating power factor correction (PFC) at the AC mains, this charger surpasses traditional setups with its streamlined design and enhanced efficiency. By harmonizing Cuk and SEPIC converters during individual half cycles and integrating an output inductor on the Cuk converter side, it achieves superior performance, particularly in output current smoothing. Rigorous validation of the newly developed BLS isolated PFC converter's exemplary power quality (PQ) operation is carried out using a 48V/100Ah electric vehicle battery load. Through meticulous testing in the MATLAB/Simulink environment with fuzzy logic (FL) controllers, the charger's performance is fine-tuned. This work represents a significant leap in electric vehicle battery charging, showcasing elegance, efficiency, and engineering excellence through meticulous thoughtful design..

Keywords: PID, Fuzzy Logic, Cuk, SEPIC, bridgeless Converter.

TABLE OF CONTENTS

CHAPTER 1	1
INTRODUCTION	1
1.1 Background and Scope.....	1
1.2 Motivation	2
1.3 Reason/Justification for the Selection of the Topic	3
1.4 Relevance to National Needs	3
1.5 Advantages	4
1.6 Areas of Application	4
1.7 Thesis Outline	5
CHAPTER 2	6
LITERATURE REVIEW	6
2.1 Types of Converters.....	6
2.2 Overview of Existing Techniques in Literature	9
2.3 Unified EVs charging Strategies	9
2.3.1 Hybrid EV Charging.....	9
2.3.2 Optimization Objectives	9
2.4 Charging infrastructure categorization	12
2.5 V2g technology.....	13
CHAPTER 3	15
PROPOSED METHODOLOGY	15
3.1.1 Converter Topology Design.....	15
3.1.2 Converter Control Strategy	15
3.1.3 Simulation Studies	15
3.1.4 Optimization of Parameters	15
3.1.5 Sensitivity Analysis	15
3.1.6 Experimentation-Based Validation.....	15
3.1.7 Performance Evaluation.....	15
3.2 Configuration of the proposed isolated BLS charger, its working and control.....	16
3.2.1 Working of BLS isolated converter	17
3.2.2 Converter Control	21
CHAPTER 4	23
RESULTS	23
4.1 Simulation Results.....	23

4.2 Fuzzy logic control for current and Voltage regulation	25
4.2.1 Fuzzy Input Variables.....	25
4.2.2 Fuzzy Rules.....	26
4.2.3 Defuzzification (Centroid Method)	26
4.2.4 Fuzzy Logic Controller.....	26
4.3 Comparison of PID with Fuzzy logic controller	29
4.4 Summary.....	31
CHAPTER 5.....	32
CONCLUSION AND FUTURE WORK.....	32
5.1 Conclusion.....	32
5.2 Future Work	32
References.....

LIST OF FIGURES

Figure 1: EV's Societal Impact.....	3
Figure 2: Buck converter	6
Figure 3: Boost Converter.....	6
Figure 4: Buck-Boost converter.....	7
Figure 5: Buck-Boost converter.....	7
Figure 6: Buck-Boost converter.....	8
Figure 7: Buck-Boost converter.....	8
Figure 8: EV's incorporate ways	11
Figure 9: EV's incorporate ways	12
Figure 10: EV's Societal Impact.....	13
Figure 11: Proposed BL Cuk-SEPIC converter-based EV charger	16
Figure 12: Waveform for switching operations.....	17
Figure 13 : One of the three modes of operation for the new BLS Isolated Converter.....	17
Figure 14: One of the three modes of operation for the new BLS Isolated Converter in interval-II.....	18
Figure 15: One of the three modes of operation for the new BLS Isolated Converter in interval-III.....	20
Figure 16. One of the three modes of operation for the new BLS Isolated Converter in interval-II (-ve SEPIC mode).	21
Figure 17. One of the three modes of operation for the new BLS Isolated Converter in interval-III (-ve SEPIC mode).	21
Figure 18. The suggested BL isolated converter operates with similar gate pulses. (a) Positive half operation (Cuk mode, with inductor at output) (b) Negative half operation (Sepic mode, with diode at output).	22
Figure 19: Cuk-SEPIC mode currents and voltages.	23
Figure 20: Cuk-SEPIC switching waveforms.....	24
Figure 21: Battery current, voltage, and SOC	24
Figure 22: Battery voltage using fuzzy logic control	28
Figure 23: Battery power using fuzzy logic control	28
Figure 24: Actual current flowing through the battery for controller.....	29
Figure 25: Convergence time of the current	29
Figure 26: Actual current is flowing through the battery for both controllers	30
Figure 27: Battery voltage comparison.....	30

Figure 28: Battery power comparison 31

LIST OF TABLES

Table 1: Actual current flowing through the battery for both controllers.....	20
--	----

LIST OF ABBREVIATION

EV	Electric Vehicles
DBR	Diode Bridge Rectifier
RE	Renewable Energy
SDP	Stochastic dynamic programming
ESSs	Energy storage systems (ESSs)
SiC	Silicon carbide
GaN	Gallium nitride BPDs
BPDs	Bypass Diodes
DPFC	Digital power factor correction
DEC	Direct energy control

CHAPTER 1

INTRODUCTION

1.1 Background and Scope

Electric cars, or EVs, have attracted a lot of interest as a green and sustainable form of transportation. EV chargers must be reliable and effective as demand for EVs grows. To charge an EV's battery with DC power, grid AC power must be converted using an EV charger. How well the process charges are mostly dependent on the charger's efficiency, power density, and dependability.

Compliance with suggested rules, such as the IEC 61000-3-2 standard, is especially important for smaller cars. High-quality battery chargers must have minimal mains current distortion (THD) and sinusoidal line current [4]. However, the diode bridge rectifier (DBR)'s nonlinear behavior at the conventional battery charger input makes obtaining high-quality indices challenging. The unsatisfactory power factor(PF) and high harmonics (60%) in line with the present PQ performance in [5] violate the IEC standards that establish the battery rating and E-rickshaw specifications. To increase utility-level PQ capabilities, a conventional front-end PFC converter is placed at the rectifier output. Nonetheless, adding another converter to the typical charger increases the overall component count, reducing charger cost and performance. Furthermore, in two-stage systems, particularly for high-power applications, the use of large DC-link capacitors affects charger efficiency, weight, and dependability [6]. As a result, single-stage isolated AC-DC converters with input diode bridges are increasingly used for PFC in EV chargers [7].

The outstanding performance characteristics of the isolated Cuk-Sepic converter have made it a competitive choice for a variety of power electronic applications. It is possible to achieve high reliability and security along with high efficiency, power density, and input and output isolation. This is why an EV charger's dependability and efficiency may be improved by adding an isolated Cuk-Sepic converter. In this thesis, an integrated isolated Cuk-Sepic converter-based EV charger is built and investigated. A thorough analysis is conducted of the recommended charger's topology, control method, and power stage architecture.

The advantages of the converter over traditional converters are demonstrated by analysing its performance through simulations. The thesis also looks at how the charger's output voltage impacts how quickly and how long it takes to fully charge a battery.

Promising performance qualities have been shown by the proposed charger, which could be a solution to the growing need for EV charging applications. For a very long time, electricity has only been able to be sent in one direction via conventional networks. As a result, there is an issue with the energy only being transported in one direction.

To overcome this challenge, following three distinct approaches can be explored i.e., integrating energy storage systems (ESS) with photovoltaic generation(PVG), combining ESS with wind generation(WG), and integrating ESS into power systems. ESS can effectively support the grid during peak demand time, emergencies.

1.2 Motivation

The motivation for researching the integration of the two converters in Electric Vehicle chargers lies in enhancing the efficiency, compactness, versatility, safety, and societal impact of electric vehicle charging systems. By leveraging the converter's power flow capability, flexibility in voltage conversion, and inherent isolation, the research aims to optimize charging efficiency, reduce size and weight, ensure electrical safety, and facilitate integration with renewable energy sources. It aims at moving forward with sustainable transportation infrastructures, specifically advancing the technological challenges and exploring innovative solutions toward future EV charging infrastructure. Having isolation capability on the EV charger is essentially critical because of safety from the electrical point of view. The inherent isolation capability of Cuk-SEPIC enables it to operate within stringent standards for EV charger applications. Research is set to dwell in improving the isolation techniques and attaining the required safety regulations. Advanced converter technologies, such as the Cuk-SEPIC, for EV chargers could provide additional benefits related to electric mobility and the environment. Research Contribute toward Sustainability The research for improved energy efficiency of charging infrastructure.

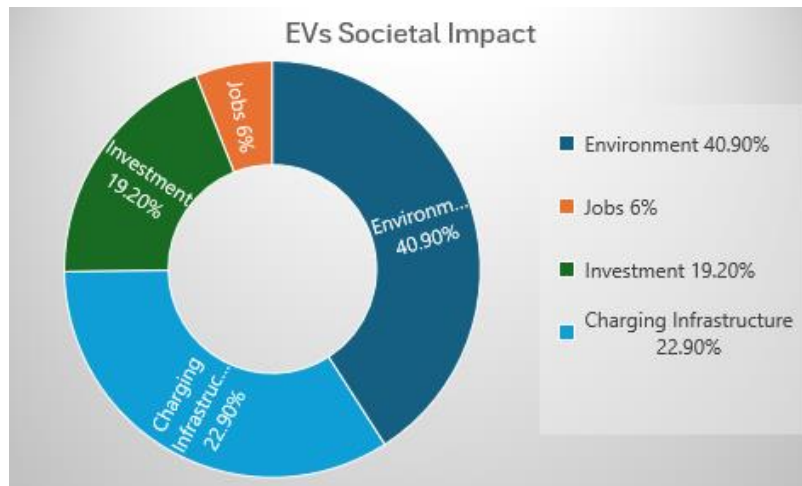


Figure 1: EV's Societal Impact

1.3 Reason/Justification for the Selection of the Topic

It justifies the research on the integration of an isolated Cuk-SEPIC converter in EV chargers since it has the potential to enhance multiple critical aspects of electric vehicle charging infrastructure. This feature enables efficiency enhancement by taking advantage of its power flow and optimized voltage conversion capabilities, which thereby take away the issue on energy losses in the process of charging. Versatility in both step-up and step-down conversions without extra transformers promotes and complements the development of universal chargers, suitable for different grid and battery voltages. As a result, this improves interoperability with ease in EV charging networks. An inbuilt isolation of the Cuk-SEPIC converter increases the electric safety, which is extremely important for the protection of vehicles and infrastructures from possible electric faults. Its compact design is space-efficient toward versatile deployment scenarios, with compatibility for renewable energy sources to allow sustainable integration into eco-friendly charging ecosystems. This subject will not only be taking the technology frontiers of power electronics further but also meeting today's market demands for effective, reliable, and environmentally conscious solutions for electric vehicle charging, thus ensuring its relevance and impact on today's evolving transport landscape.

1.4 Relevance to National Needs

It is also crucial in relevance to national needs and global imperatives to study the integration of an isolated Cuk-SEPIC converter into EV chargers. Reducing dependency on fossil fuels and guaranteeing the security of energy are an energy security issue for most countries. Electric

vehicles are the foremost important players in that transition, using electricity obtained from all sources, renewable or not.

1.5 Advantages

The following are the benefits accompanying the integration of an isolated Cuk-SEPIC converter in EV chargers:

Efficiency: Reduces energy losses during the charging process, improving overall efficiency.

Versatility: Acts in both up and down voltage conversion with no need for transformers, rendering it effective for a range of grid and battery voltage uses.

Safety: Provides inherent galvanic isolation between input and output, making vehicles and infrastructure electrically safe.

Compact Design: Occupies less footprint relative to other isolated converter topologies—space-saving design. Suitable for space-constrained environments.

Environmental Sustainability: Facilitates the integration of renewable energy sources, promoting eco-friendly charging solutions.

Technological Innovation: Advances in power electronics technology contribute to technological leadership and competitiveness.

Interoperability: Leads to universal chargers effective in charging different kinds of EVs, enhancing market scalability.

Compliance: Meets regulatory standards for energy efficiency, safety, and interoperability in EV charging infrastructure.

1.6 Areas of Application

The isolated Cuk-SEPIC converter integrated in this framework has wide applications across both sectors and environments. It is a crucial component in public EV charging stations due to its capability to support efficient and safe charging in towns, parking lots, and highway locations. Its flexibility supports both different EV designs and battery configurations used in commercial and workplace charging facilities. The converter enables convenient home charging solutions in residential settings, facilitating the transition to electric vehicle technology. Additionally, it supports fleet management for electric buses, delivery vehicles, and other fleet applications, optimizing energy charging.

Moreover, it plays a crucial role in fleet management, optimizing charging efficiency for electric buses, delivery vehicles, and other fleet applications.

1.7 Thesis Outline

Here's how everything is structured: Section II delves into charger configuration, operation details, & battery management. Section III gets into designing our proposed BLS converter more closely. Then Section IV shares what we found out through simulation results so you get a full picture of our research journey! Finally, Section V wraps it all up with nice conclusions about what we learned and why it matters.

CHAPTER 2

LITERATURE REVIEW

2.1 Types of Converters

1. Buck Converter:

The buck converter is primarily used to reduce DC voltage levels efficiently. It operates by varying the percentage of time a switch is on or off, ensuring that the output voltage is always lower than the input voltage, making it ideal for battery applications.

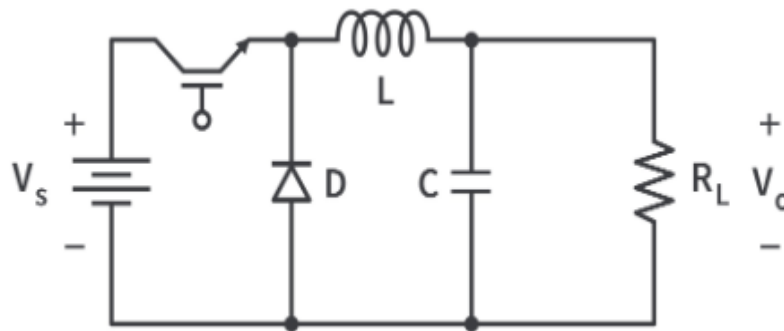


Figure 2: Buck converter

2. Boost Converter :

The buck-boost converter allows versatile voltage conversion, capable of stepping up and stepping down DC voltages. It efficiently adjusts the output polarity relative to the input, making it suitable for scenarios with variable input voltage.

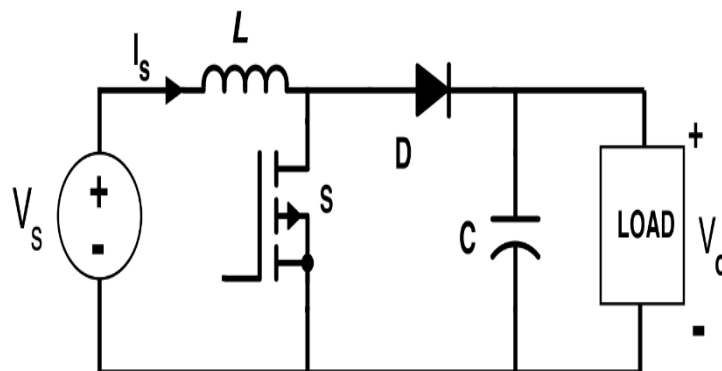


Figure 3: Boost Converter

3. Buck-Boost Converter:

The buck-boost converter provides versatility in voltage conversion, capable of both stepping up and stepping down DC voltages. It efficiently adjusts output polarity relative to the input, making it suitable for variable input voltage scenarios.

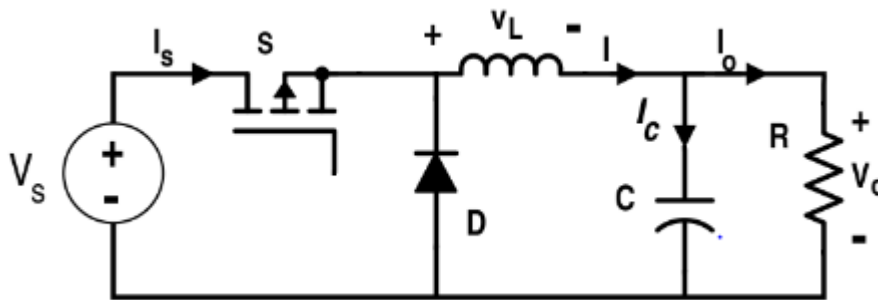


Figure 4: Buck-Boost converter

4. Cuk Converter:

The Cuk converter operates without electrical isolation, offering continuous input and output currents during voltage conversion. It accommodates both step-up and step-down conversions effectively.

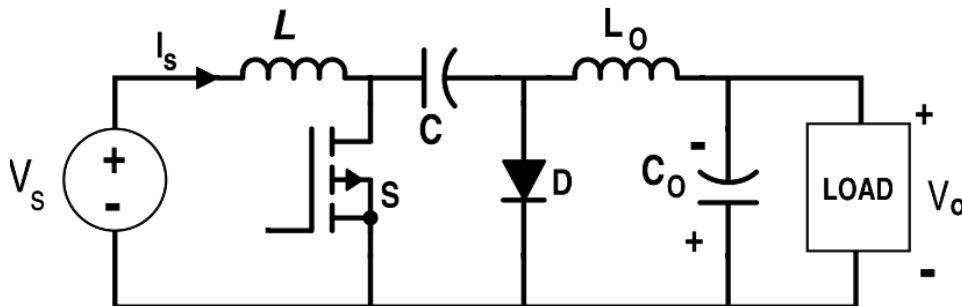


Figure 5: Buck-Boost converter

5. Flyback Converter:

Employing a transformer for isolation, the flyback converter stores energy in the transformer during switch-on periods and transfers it to the output during switch-off periods. It is suitable for applications requiring isolation between input and output.

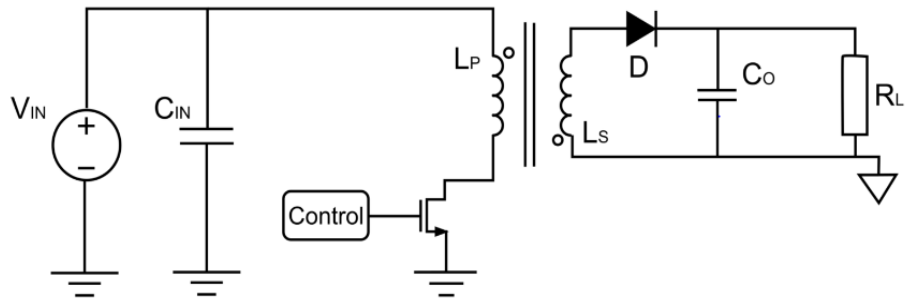


Figure 6: Buck-Boost converter

6. SEPIC Converter (Single-Ended Primary Inductor Converter):

The SEPIC converter facilitates non-inverting voltage conversion from a DC input to an adjustable DC output, accommodating varying input voltages effectively.

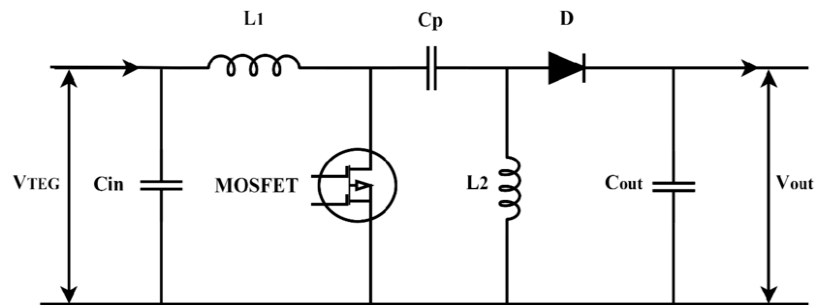


Figure 7: Buck-Boost converter

7. Full-Bridge Converter:

Utilizing a bridge topology with four switches, the full-bridge converter efficiently converts DC voltage for high-power applications. It finds extensive use in industrial power supplies and electric vehicle charging systems.

8. Half-Bridge Converter:

The half-bridge converter employs two switches for medium-power DC voltage conversion, emphasizing simplicity and cost-effectiveness.

9. Push-Pull Converter: Using a transformer and two switches, the push-pull converter efficiently converts DC voltage while minimizing electromagnetic interference. It is crucial in applications where high efficiency and low noise are paramount.

2.2 Overview of Existing Techniques in Literature

Advanced EV charging reduces transformer loads, thereby lowering energy costs and decreasing the CO₂ ratio through optimal EV charging practices, which is beneficial for clients and helps maintain power system stability [3]. Currently, AU is employed for managing the central device and connecting EV's to the aggregator units manage load aggregation and provide a flexible framework for enhancing EV performance, accommodating diverse charging methods efficiently. Additionally, UA delivers secondary services and enhances the overall benefits of the EV network.

2.3 Unified EVs charging Strategies

The chapter delves into the control strategies of unit aggregators and the methodologies for EV charging [5]. It discusses how unit aggregators gather EV charging data, which is crucial for managing power system protection [6] and influencing grid stability. Control demand forecasting is enhanced through optimization techniques alongside other beneficial methodologies.

2.3.1 Hybrid EV Charging

Hybrid EV charging is a combination of different techniques to support the optimal charging process . Centralized EV charging, on the other hand, involves a central aggregator that collects all choices and makes the best charging decision based on comprehensive client requirements. This enhances the effectiveness of the central aggregator by ensuring decisions are based on effective data aggregation.

2.3.2 Optimization Objectives

Considerable research focuses on improving and optimizing EV charging systems, incorporating various techniques like sustainable power resource resolution and allocation . Advanced methods for EV charging significantly reduce battery storage power crises and improve distribution system quality compared to Internal Combustion Engine Vehicles (ICEVs). ICEVs experience substantial energy crises even when idle, in contrast to advanced EV charging, where distribution is highly effective with minimal or no power crises.

The rising demand for EVs has created a need for well-designed, effective, and reliable chargers that convert grid AC power into DC for EV batteries. Understanding EV charger technologies and their components is crucial for optimizing operation. Key requirements

include efficiency to reduce energy losses during charging, power density for compactness, and reliability to ensure consistent performance when charging EV batteries. Innovations in materials, such as gallium nitride (GaN) and silicon carbide (SiC)-based semiconductors, reduce losses while increasing power density. The use of sophisticated control algorithms further improves charger efficiency and reliability; while sensing and monitoring systems ensure chargers operate within defined parameters, optimizing the implementation of EV charging infrastructure as part of sustainable transportation solutions.

In summary, advancements in EV charger technology have improved efficiency, density, and reliability to support the growing EV market. These innovations pave the way for sustainable transportation solutions and enhanced grid stability. References review different onboard EV chargers with single-phase PFC converters suitable for high-power, compact applications. Interleaved PFC designs optimize high-power efficiency, while soft-switching techniques reduce EMI and inductance. Challenges in heat dissipation persist with rectifier-fed chargers, hindering size reductions. Single-stage resonant converters [11] promise lower EMI and switching losses, but complexities arise from component selection across different voltages. Boost-FBLLC converters [12] introduce added complexity, and unidirectional charging methods [13] focus on simplicity and power density. Buck-boost converters [14, 15] manage varying mains voltages efficiently but lack isolation and suffer efficiency losses in single-stage applications. Innovative approaches like Cuk converters [17, 18] mitigate ripple and improve power quality, albeit with EMI challenges and gate driver requirements. SEPIC converters [19] address current discontinuity issues but face practical challenges in isolated configurations.

The chapter emphasizes DC-DC converter types and EV charging topologies, providing comprehensive insights into optimizing EV charging systems. Shu and Jirutitijaroen [1] proposed policies in 2014 for optimal operation of energy storage systems, focusing on profit maximization through uncertainty resolution in electricity bills and wind generation using stochastic dynamic programming (SDP). The research rate on renewable energy resources and electrical vehicles is increasing day by day shown in figure below. We have a brief review of different enhancement techniques, goals and techniques utilized for charging process of EVs and the fundamental commitments will give the abridged as pursues:

As shown in Figure 8 below, incorporate ways of EVs are shown. Different abbreviations for charging techniques have also been used. Also, the distinctive advancement techniques are also discussed.

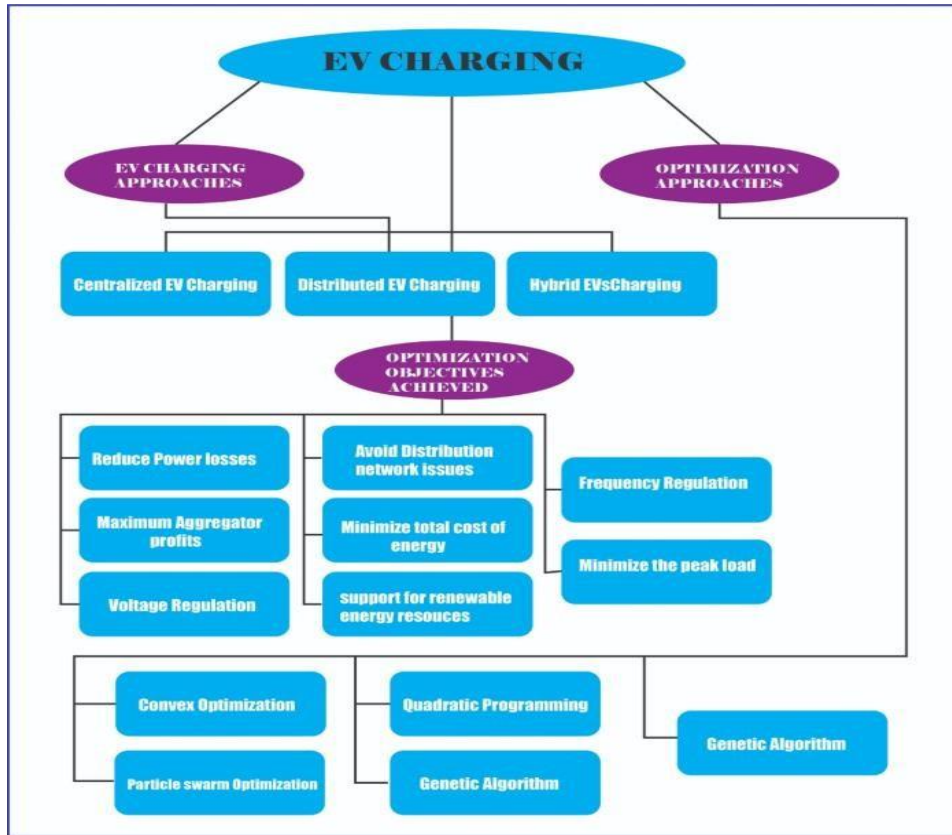


Figure 8: EV's incorporate ways

The proposed system focuses on two primary conditions: normal operational costs of microgrids and load reduction during unplanned events initiated by the main grid. EVs (electric vehicles) are identified as an emerging technology aimed at addressing these challenges. In the future, electricity consumption is projected to decrease relative to electricity generation due to consumers sharing surplus power from renewable energy sources with the distribution network, thus fostering new business opportunities. Research into renewable energy resources is progressively intensifying.

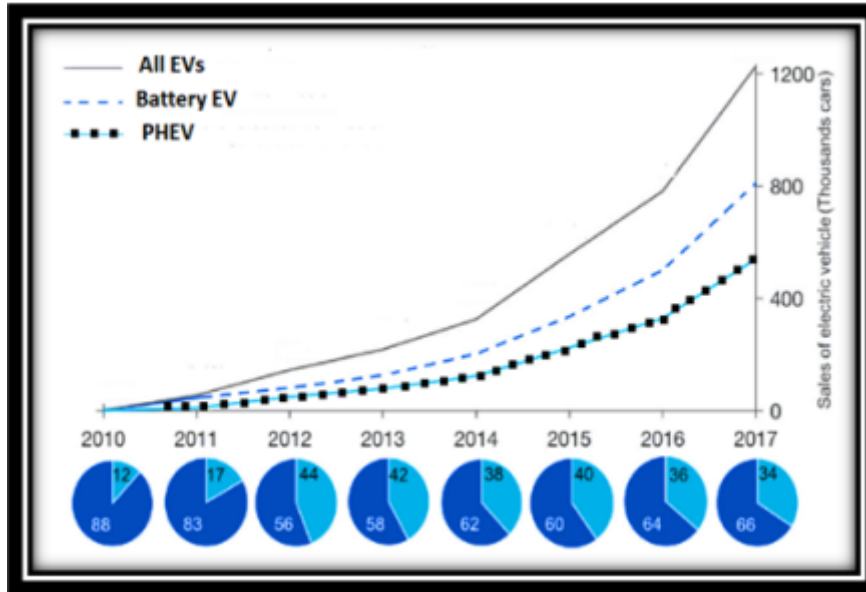


Figure 9: EV's incorporate ways

In 2017, D. Sharma, S. Singh, J. Lin and E Foruzan [12] have proposed the required power exchange with distributed power systems (DESSs) in their power / most permitted power to charge or discharge functions used as interchangeable information between various associated battery agents and DESS. First, a comprehensive information retrieval system is proposed based on understanding the consequences of cyber-attacks on information.

2.4 Charging infrastructure categorization

Charging frameworks can be divided into multiple sorts according to control levels and charging system types [10]. These consist of systems that are partly open, closed, and open [14]. The figure below provides examples of the various frameworks that have been discussed.



Figure 10: EV’s Societal Impact

2.5 V2g technology

This process alleviates stress on distribution networks and improves their overall efficiency by discharging EV batteries during peak demand periods. V2G applications are relatively new but promising in power systems, facilitating bidirectional power flow between vehicles and the grid.

In unidirectional V2G setups, power flows only from the grid to the electric vehicle. This technology enables EVs equipped with unidirectional chargers to charge from the grid but not discharge power back. It is appealing due to its simpler infrastructure requirements, needing only a dedicated port, hardware, and battery management system.

This approach enhances grid performance by stabilizing operations and serving as a reliable reserve during peak demand. To promote V2G adoption, smart trading policies are being implemented. Table 1 provides data on voltage, current, and real power for various battery charging methods, emphasizing the use of single-stage converters to minimize weight, size, cost, and losses [17].

Isolated high-frequency (HF) transformers can fulfill isolation requirements [20], and phase angle control of current enables the delivery or extraction of reactive power with unidirectional chargers. Implementation of unidirectional V2G typically avoids additional transmission expenses in many regions [19], despite offering fewer advantages compared to bidirectional V2G algorithms.

Bidirectional V2G allows power to flow in both directions between the electric vehicle and utility grid. Comparative studies highlight several advantages of bidirectional V2G over unidirectional setups. Bidirectional chargers involve two stages: an AC to DC stage capable of power factor (P.F) improvement through harmonic reduction, and a DC-to-DC converter for electric vehicle control.

CHAPTER 3

PROPOSED METHODOLOGY

This research work proposes a novel procedure of integration of two bridgeless isolated converters that is Cuk converter and SEPIC converter-based EV charger, which is controlled by PID controller as well as the Fuzzy logic controller(FLC).

3.1 Theory and Mathematical Concept

3.1.1 Converter Topology Design

First, design an isolated bridgeless Cuk-SEP converter for a special purpose only, which is the charger for electric vehicles. We chose the switches, capacitors, and stuff like inductors in the circuit. Then we calculate their values to meet some standards. Next is to construct a circuit model in tools like MATLAB/Simulink or PSIM. All selected components are designed within these components of the converter.

3.1.2 Converter Control Strategy

Next comes the control strategy, which helps us regulate the functioning of the converter while keeping it at the desired output voltage and current levels. We look at several control techniques like proportional-integral (PI) control or fuzzy logic control, which would help us to get better performance.

3.1.3 Simulation Studies

After completing the control strategy, we carry out a large number of simulation studies. These research works verify the performance of the converter under varying conditions. Efficiency, power factor, voltage ripple, and current ripple are some things that we are after.

3.1.4 Optimization of Parameters

The parameters are optimized after learning from simulations; thus, the control strategy and component values are fine-tuned. Everything is to ensure the converter works as best as can be.

3.1.5 Sensitivity Analysis

Then sensitivity analysis is also done. This allows us to observe the behavior of the converter in different situations—for example, with a changing input voltage or variations in the load.

3.1.6 Performance Evaluation

Lastly, we evaluate everything using data from both our simulations & tests, we thoroughly check how well the isolated bridgeless Cuk-SEPIC converter performs. This includes looking

at efficiency, power factor, voltage ripple, and current ripple characteristics. It's an exciting journey of exploration.

3.2 Configuration of the proposed isolated BLS charger, its working and control

This is particularly true when the SEPIC topology is harmoniously integrated with another topology that ensures a continuous output current, such as the Cuk converter. This synergistic combination of these two topologies emerges as a prevalent choice for enhancing PQ in EV chargers. In the pursuit of maximizing charger efficiency, numerous BLS Power PFC converter topologies with isolation have been extensively documented in the literature. The circuit derivation of a novel BLS Cuk-SEPIC converter is extrapolated from the conventional Cuk and SEPIC converters, as illustrated in Figure 11.

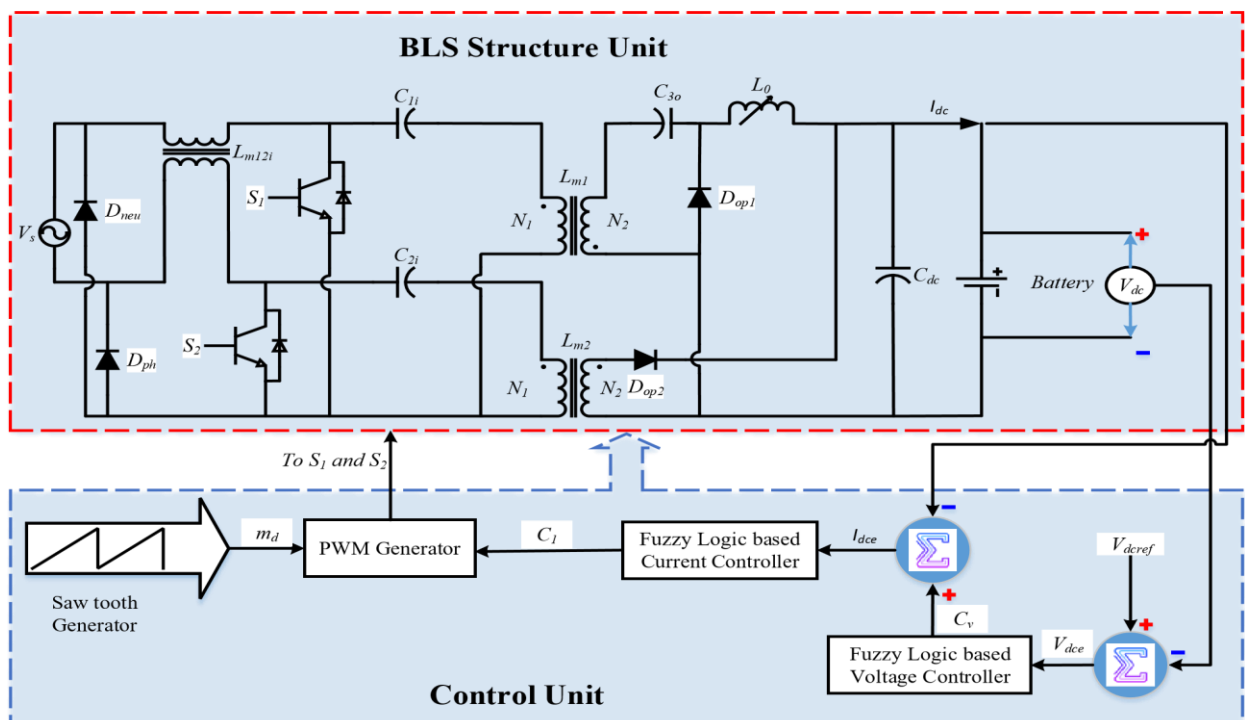


Figure 11: Proposed BL Cuk-SEPIC converter-based EV charger

Figure 11 shows the configuration of the proposed BLS converter system, which is intended to improve the PQ of a battery charger. The converter operates in DSM, resulting in unity power factor (UPF) performance under steady-state conditions and across a wide range of operating line voltages and loads. This novel configuration is the result of combining isolated Cuk and SEPIC converters, each operating independently during separate half cycles. The Cuk converter uses a semi conducting switch S_1 , an intermediate capacitor C_{11} , a transformer magnetizing inductance L_{m1} , and an output diode D_{op1} in the +ve half line. During the -ve

half-line, the SEPIC converter uses the S2, intermediate capacitor C2i, magnetizing inductance of the transformer (Lm2), and output diode Dop2.

3.2.1 Working of BLS isolated converter

The isolated BLS converter is configured in DCM, with a discontinuity in the current through Lm1,2, at the switching cycle ends. The converter operates in three distinct modes, with primary operations displayed in Cuk mode (+ve half cycle) and SEPIC mode (-ve half cycle) as shown in Figure 12 below.

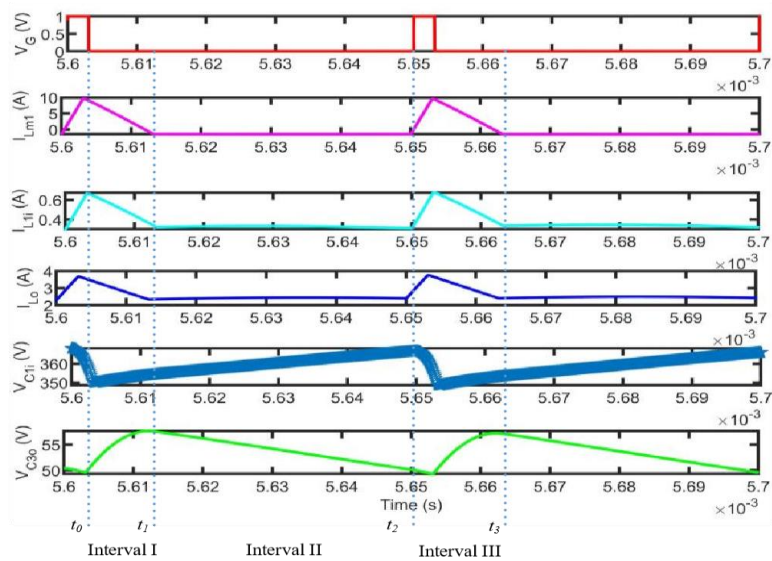


Figure 12: Waveform for switching operations

Interval-I [$t_0 - t_1$] activates switch S1. As the power source charges the i/p inductance Lli, the current I flowing through it grows linear. Figure 13 shows that the voltage across the intermediate capacitance vC1i declines as energy is stored in the Lm1. During this interval, the o/p diode Dop1 is reverse-biased.

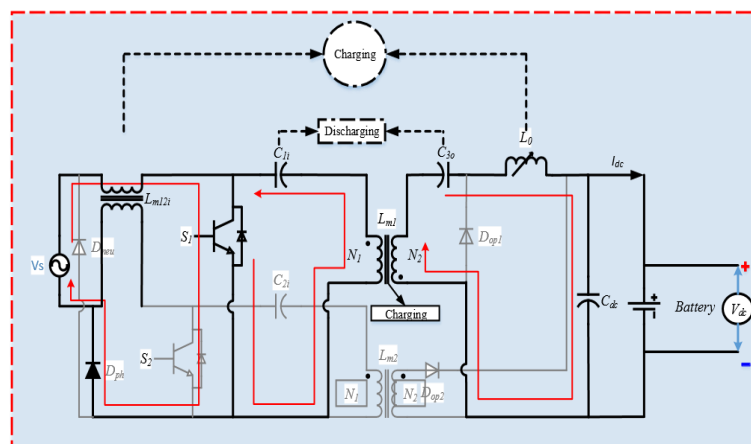


Figure 13 : One of the three modes of operation for the new BLS Isolated Converter

The energy transfer to the capacitor C3o discharges through the output inductance Lo, which then provides the necessary charging current to the battery. The currents in inductors L1i, Lm1, and Lo are represented as follows:

$$\begin{aligned}
 i_{L_{1i}}(t) &= I_{L_{1i}}(t_0) + \frac{V_{in}}{L_{1i}}(t - t_0) \text{ for } t_0 \leq t \leq DT_s \\
 i_{L_{m1}}(t) &= I_{L_{m1}}(t_0) + \frac{V_{C1i}}{L_{m1}}(t - t_0) = I_{L_{m1}}(t_0) + \\
 &\quad \frac{V_{in}}{L_{m1}}(t - t_0) \\
 i_{L_o}(t) &= I_{L_o}(t_0) + \frac{nV_{C1i} + V_{C3o} - V_{dc}}{L_o}(t - t_0) \\
 &= I_{L_o}(t_0) + \frac{nV_{in}}{L_o}(t - t_0)
 \end{aligned}$$

The current through switch $i_{s1}(t)$ is determined using equation (1) as follows:

$$\begin{aligned}
 i_{s1}(t) &= i_{L_{1i}}(t) + i_{L_{m1}}(t) + ni_{L_o}(t) \\
 &= I_{L_{1i}}(t_0) + I_{L_{m1}}(t_0) + nI_{L_o}(t_0) + \\
 &\quad \frac{V_{in}}{(L_{1i} + L_{m1}) \square (L_o/n^2)}(t - t_0) \\
 &= I_{L_{1i}}(t_0) + I_{L_{m1}}(t_0) + nI_{L_o}(t_0) + \\
 &\quad \frac{V_{in}}{(L_{1i} + L_{m1}) \square (L_o/n^2)}DT_s \\
 i_{Dop1} &= 0
 \end{aligned}$$

In this context, D represents the turn-on ratio, ensuring the maintenance of the necessary 65V at the proposed converter's output, considering the specified transformer turn ratio ($\frac{N_2}{N_1} = n$). T_s corresponds to a switching interval (complete one), V_{in} stands for the peak grid-rated voltage, and i_{L_o} denotes the current flowing through L_o .

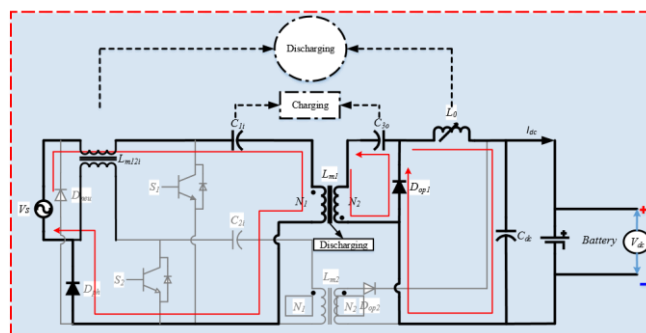


Figure 14: One of the three modes of operation for the new BLS Isolated Converter in interval-II

Interval-II [$t_1 - t_2$]: As depicted in Fig. 14 above, this phase initiates now t_l when switch S1 is turned off, enabling the conductivity of the output diode Dop1. The output diode Dop1 receives the magnetizing inductance Lm1's release of stored energy via the capacitor C1i, while the capacitor C3o charges at the secondary winding of the high-frequency transformer (HFT). The equation that results from applying volt-sec balance to L1i and Lm1 is as follows:

$$V_{in}D + (V_{in} - V_{C1i}) D_1 = 0 \quad (3)$$

This equation gives

$$V_{C1i} = \frac{D_1 + D}{D_1} V_{in} \quad (4)$$

Additionally, another equation $V_{C1i}D + \left(\frac{V_{dc}}{n}\right) D_1 = 0$ leads to $V_{dc} = -\frac{nD}{D_1} V_{C1i} = -\frac{nD}{D_1} \left(\frac{D_1 + D}{D_1}\right) V_{in} = -\frac{nD}{D_1} V_{in} - \frac{nD^2}{D_1^2} V_{in}$.

Neglecting the squared terms for D and D_1 , we simplify to

$$V_{dc} = -\frac{nD}{D_1} V_{C1i} = -\frac{nD}{D_1} V_{in} \quad (5)$$

From equations (4) and (5), the currents in L_{1i} , L_{m1} , and L_o can be represented as:

$$\begin{aligned} i_{L_{1i}}(t) &= I_{L_{1i}}(t_0) + \frac{V_{in}}{L_{1i}} DT_s + \frac{V_{in} - V_{C1i}}{L_{1i}} (t - t_1) \\ &= I_{L_{1i}}(t_0) + \frac{V_{in}}{L_{1i}} DT_s + \frac{nV_{dc}}{L_{1i}} (t - t_1) \end{aligned} \quad (6)$$

D_1 denotes the length of time of the converter's OFF condition, while V_{c1i} , V_{c3o} denotes the voltage C_{1i} , C_{3o} in the positive line cycle.

$$\begin{aligned} i_{L_{m1}}(t) &= I_{L_{m1}}(t_0) + \frac{V_{in}}{L_{m1}} DT_s + \frac{V_{dc}/n}{L_{m1}} (t - t_l) \\ i_{L_o}(t) &= I_{L_o}(t_0) + \frac{nV_{in}}{L_o} DT_s + \frac{V_{dc}}{L_o} (t - t_l) \\ i_{Dop1} &= i_{L_o} - i_{C3o} = i_{L_o} + (i_{L_{1i}} + i_{L_{m1}}) / n \end{aligned} \quad (7)$$

$$\begin{aligned} i_{Dop1}(t) &= \frac{I_{L_{1i}}(t_0) + I_{L_{m1}}(t_0)}{n} + I_{L_o}(t_0) + \\ &\frac{V_{in}}{n(L_{1i} + L_{m1}) \square (L_o/n)} (t - t_0) - \frac{V_{dc}/n}{n(L_{1i} + L_{m1}) \square (L_o/n)} \\ &(t - t_l) \\ &= \frac{I_{L_{1i}}(t_0) + I_{L_{m1}}(t_0)}{n} + I_{L_o}(t_0) + \\ &\frac{nV_{in}}{n^2(L_{1i} + L_{m1}) \square L_o} DT_s - \frac{V_{dc}}{n^2(L_{1i} + L_{m1}) \square L_o} D_1 T_s \end{aligned} \quad (8)$$

$$\begin{aligned}
i_{L_{1i}}(t) &= I_{L_{1i}}(t_0) + \frac{V_{in}}{L_{1i}}DT_s + \frac{V_{in} - V_{C1i}}{L_{1i}}(t - t_2) \\
&= I_{L_{1i}}(t_0) + \frac{V_{in}}{L_{1i}}DT_s + \frac{V_{in} - V_{C1i}}{L_{1i}}(t - t_2) \\
i_{L_o}(t) &= I_{L_o}(t_0) + \frac{nV_{in}}{L_o}DT_s - \frac{V_{dc}}{L_o}(t - t_2) \quad (9)
\end{aligned}$$

For $(D)(T_s) + (D_1)(T_s) = t_2 \leq t \leq T_s$, $i_{s1} = 0; i_{Dol} = 0$

Interval-III [$t_2 - t_3$]: In this period, the switch S_l stays in the OFF state. The current traversing the three inductances is directed in a manner that interrupts conduction through the output diode, D_{ol} , causing i_{Dol} to drop to zero. The necessary load current is then provided by the output capacitor, C_{dc} , as illustrated in Figure 15, capturing this operational state.

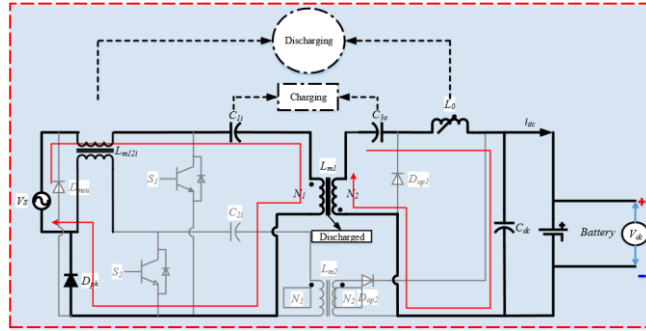


Figure 15: One of the three modes of operation for the new BLS Isolated Converter in interval-III

Likewise, Figures 16, 17, and 18 provide a visual representation of the switching sequence and functioning in the SEPIC side of the charger when operating in Discontinuous Conduction Mode. The corresponding switching wave formation, depicts various voltages across and currents are showcased in Figure 13.

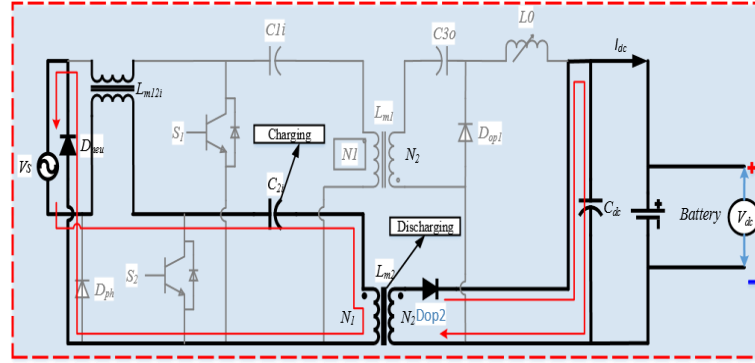


Figure 16. One of the three modes of operation for the new BLS Isolated Converter in interval-II (-ve SEPIC mode).

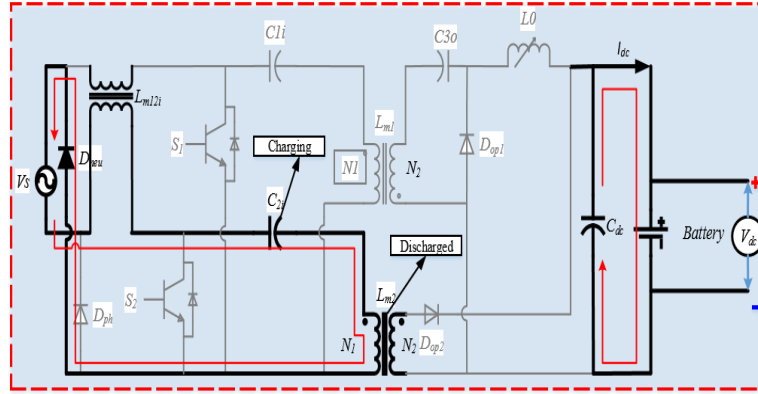


Figure 17. One of the three modes of operation for the new BLS Isolated Converter in interval-III (-ve SEPIC mode).

3.2.2 Converter Control

The suggested charger, based on the BLS isolated converter, uses a pair of semiconductor switches that operate simultaneously throughout a single switching cycle. To ensure that the two PFC switches produce comparable pulses, a cascaded FL controller is used.

The continuous profile of current monitors the I_{dc} that passes through the battery. The error I_{dce} is calculated by comparing this current to the set reference current I_{dcref} , which is subsequently sent to the FL. In this scenario, the current can be expressed at each given instant m as follows:

$$I_{dce}(m) = I_{dcref}(m) - I_{dc}(m) \quad (10)$$

During CC mode, a voltage-FL controller determines the battery's current reference, I_{dcref} . The current FL controller's output is represented by another control signal, C_I . Constant Current (CC) mode provides a continuous battery current from the mains across the state of charge (SOC) range up to 80%. Constant Voltage (CV) mode is selected by the battery control when the SOC surpasses 80%, and the voltage FL controller replaces the current controller. The grid

current drops as the battery hits its full state of charge (SOC) limit because it is drawing less current.

Now for the voltage, the error term can be produced by comparing the actual voltage of the battery V_{dc} and the reference one V_{dcref} at m^{th} instant as follows:

$$V_{dce}(m) = V_{dcref}(m) - V_{dc}(m) \quad (11)$$

The voltage error, V_{dce} , produces another control input (C_v). To create gate signals for the PF, compare the control signal C_I to a sawtooth wave.

In comparison to interleaved converters, the control method for the proposed system. Both switches use comparable pulses but work independently of one other. One switch operates during +ve half-cycle, while the other operates during -ve half-cycle. It is worth noting that, even if both switches in the BL converter receive pulses simultaneously (with no phase delay), the configuration of line diodes D_p and D_n , as well as the polarity of the source voltage, ensures that only one cell, either in the positive or negative half-cycle, operates at any given time. Figures 18 (a) and (b) demonstrate the current path, which helps clarify the operational notion.

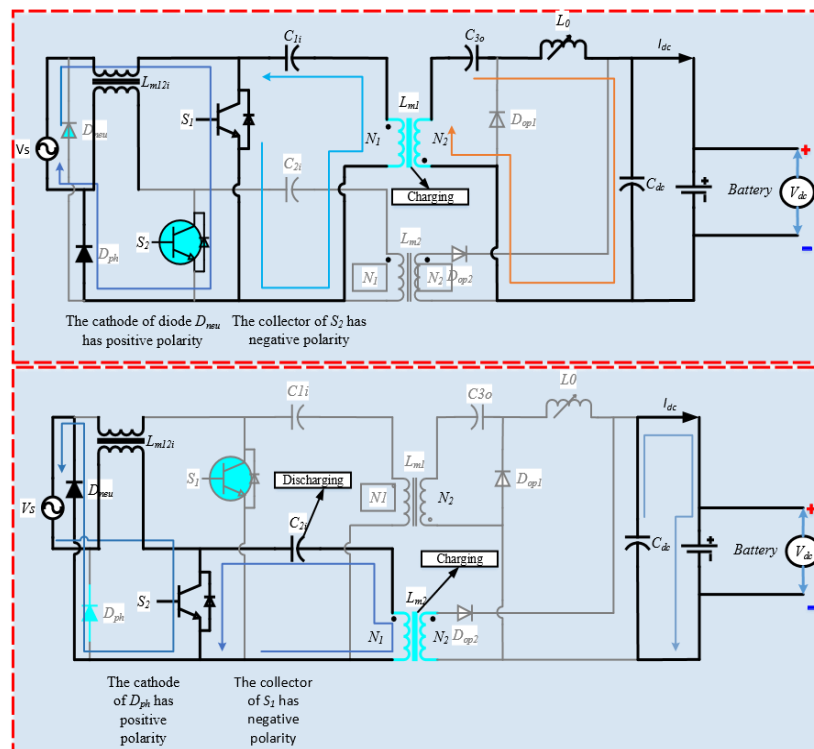


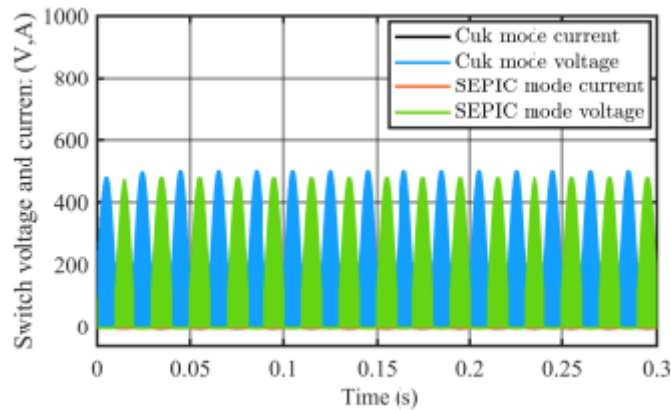
Figure 18. The suggested BL isolated converter operates with similar gate pulses. (a) +ve half operation (Cuk mode, with L at o/p) (b) -ve half operation (Sepic mode, with diode at o/p).

CHAPTER 4

RESULTS

4.1 Simulation Results

The simulation had been done on MATLAB/Simulink. The time duration for the simulation is 0.3 seconds. The effectiveness of the proposed BLS isolated converter charger, designed to enhance PQ, has been verified and contrasted using a distinct controller i.e. the fuzzy logic controller(FLC). The operational robustness of the envisaged isolated converter charger is visually demonstrated in Figure 11. The recommended converter operates in a Bridgeless configuration, utilizing operations of both the converters i.e. Cuk-Sepic as shown in Figure 19, ensuring improved performance and stability.



Figure

Figure 19: Cuk-SEPIC mode currents and voltages.

As shown in Figure 20, the primary side capacitors exhibit satisfactory performance, maintaining a consistent voltage across them throughout the complete switching cycles. Capacitors C1 and C2 operate in Cuk and SEPIC modes during the both +ve and -ve cycles. Additionally, the waveforms of the input inductor current in Continuous.

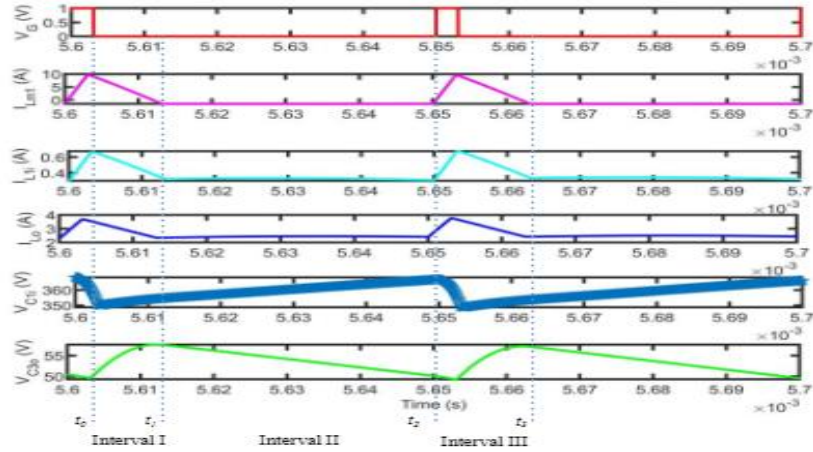


Figure 20: Cuk-SEPIC switching waveforms

The output side of the system i.e., battery has the state of charge SOC%, the battery current(A) and the battery voltage(V) is shown in Figure 21, shows the battery current, voltage, and state of charge (SOC). The ripple in current varies between 1.5 and 2A, which is within an acceptable range. Because of the inclusion of an inductor at the output, the ripple variance is small in comparison to an isolated SEPIC converter, which enhances battery life and health over time.

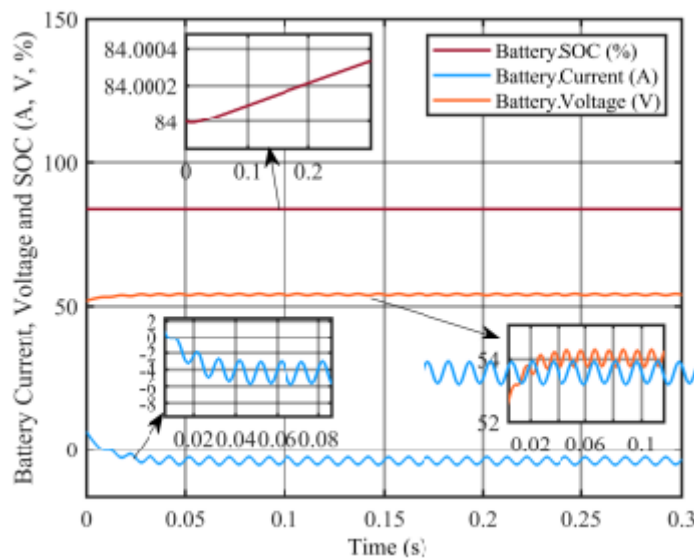


Figure 21: Battery current, voltage, and SOC

One of the way of output inductance (L_0) using the variable inductance method: This can be done by varying the duty cycle (D) so L_0 will vary accordingly, and the change in inductance value will correspondingly improve the gain (G):

$$\begin{aligned}
L_0 &= \frac{V_{dc}\{1 - D(t)\}}{\Delta I_{L_0}(t) f_s} \\
&= \frac{V_{dc} D(t)}{k I_{dc} f_s} \\
&= \left(\frac{R_{in} V_{dc}}{k V_{in}(t) f_s} \right) \\
G &= \frac{V_{dc}}{V_{in}} \\
G &= \frac{N_2 D}{N_1 (1 - D)} \\
G &= \frac{N_2 D}{N_1 (1 - D)} \\
L_0 &= \frac{R_{in} G}{k f_s}
\end{aligned}$$

$$\begin{aligned}
G &= \frac{L_0 k f_s}{R_{in}} \\
L_0 &= 795.8 \Delta 4\pi \\
L_0 &= 895.854 H. \\
L_0 &= 695.85 \mu H \\
k &= 0.2 \\
f_s &= 20,000 \\
R &= 0.05 \Omega.
\end{aligned}$$

$$\begin{aligned}
G &= \frac{N_2 \Delta}{N_1 (1 - D)} \\
L_0 &= \frac{R_{in} G}{k f_s} \\
G &= \frac{L_0 k f_s}{R_{in}}
\end{aligned}$$

4.2 Fuzzy logic control for current and Voltage regulation

Let V_{dcref} (m) denote the voltage error and I_{dref} (m) denote the current error. These errors are used as inputs to the fuzzy logic controller to determine the duty cycle (D) of the converter.

4.2.1 Fuzzy Input Variables

Define fuzzy sets for V_{error} and I_{error} :

- Voltage error:
 - Negative Big (NB)
 - Negative Medium (NM)
 - Zero (Z)
 - Positive Medium (PM)

➤ Positive Big (PB)

• Current error:

➤ Negative Big (NB)

➤ Negative Medium (NM)

➤ Zero (Z)

➤ Positive Medium (PM)

➤ Positive Big (PB)

4.2.2 Fuzzy Rules

Define fuzzy rules relating input variables to the duty cycle:

- Rule 1: If Verror is PB and Ierror is NB, then D is NB.
- Rule 2: If Verror is PM and Ierror is NB, then D is NM.
- Rule 3: If Verror is Z and Ierror is Z, then D is Z.
- Rule 4: If Verror is NM and Ierror is PM, then D is PM.
- Rule 5: If Verror is NB and Ierror is PB, then D is PB

4.2.3 Defuzzification (Centroid Method)

To obtain a crisp value of the duty cycle (D), we use the centroid method:

$$D = \frac{\sum_i \text{membership}(D_i) \times D_i}{\sum_i \text{membership}(D_i)}$$

Where D_i represents each possible duty cycle value and membership (D_i) is the membership function value for each fuzzy set D_i .

4.2.4 Fuzzy Logic Controller

MATLAB built-in Fuzzy Logic controller block is used to regulate the battery current. The following steps explain the process of regulation of current for controlling the converter switches.

4.2.4.1 Error Calculation: Compute the error (e) as the difference between the reference current (I_{ref}) and the actual current

(I_{dc}):

$$e = I_{\text{ref}} - I_{\text{dc}}$$

4.2.4.2 Linguistic Variable Assignment: Determine linguistic variables to describe the error, such as Negative Large (NL), Zero (Z), and Positive Large (PL).

4.2.4.3 Membership Function Evaluation: Given the error, evaluate the degree of membership for each linguistic variable utilizing triangular or trapezoidal membership functions. Find:

- $\mu_{NL}(e)$: Degree of membership for Negative Large
- $\mu_Z(e)$: Degree of membership for Zero

4.2.4.4 Fuzzy Rule Application Represent the fuzzy rules as a function of combinations of the linguistic variables and the resulting degree of membership.

Rule 1: IF e is NL, THEN output is NL.

Rule 2: IF e is Z, THEN output is Z.

Rule 3: IF e is PL, THEN output is PL.

4.2.4.5 Aggregation of Fuzzy Outputs:

Merge the fuzzy output sets generated by the fuzzy rules to obtain a composite fuzzy output.

4.2.4.6 Defuzzification:

Use a defuzzification method (e.g., centroid method) to get a crisp control action from the fuzzy output. Finally, determine the correct type of control signal or change needed for the system through the defuzzied output

4.2.4.7 Control Signal Application:

Implement the computing control action to regulate the current in the electrical system. This may involve adjusting parameters such as the duty cycle of a PWM signal or other control signals.

4.2.4.8 Monitoring and Iteration:

Continuously monitor the system's performance. If needed, adjust the fuzzy logic controller parameters or rules based on feedback to improve the control system's effectiveness.

The simulation studies are carried out in MATLAB/Simulink environment. The time duration for the simulation is 0.3 seconds. The effectiveness of the proposed BLS isolated converter charger, designed to enhance PQ, has been verified and contrasted using a distinct controller: the fuzzy logic controller. The operational robustness of the envisaged isolated converter charger is visually demonstrated in Figure 11.

The recommended converter operates in a Bridgeless configuration, utilizing Cuk operation in the positive half and SEPIC operation in the negative half of the line, ensuring improved

performance and stability. As shown in Figure 20, the primary side capacitors exhibit satisfactory performance, maintaining a consistent voltage across them throughout the entire switching cycle.

Following were the results achieved by using fuzzy logic controller technique. Figure 22 depicts the voltage of the battery using FLC,

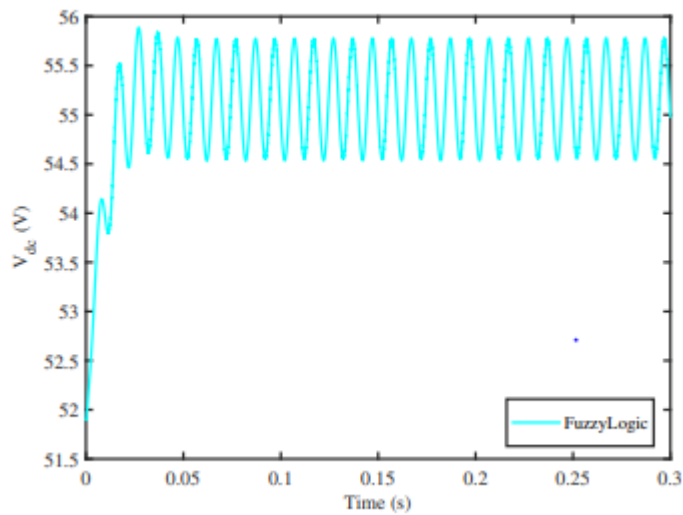


Figure 22: Battery voltage using fuzzy logic control

Figure 23 shows the results of the battery power of the system using fuzzy logic controlling technique, and in Figure 16, there is Actual current flowing through the battery for this controller.

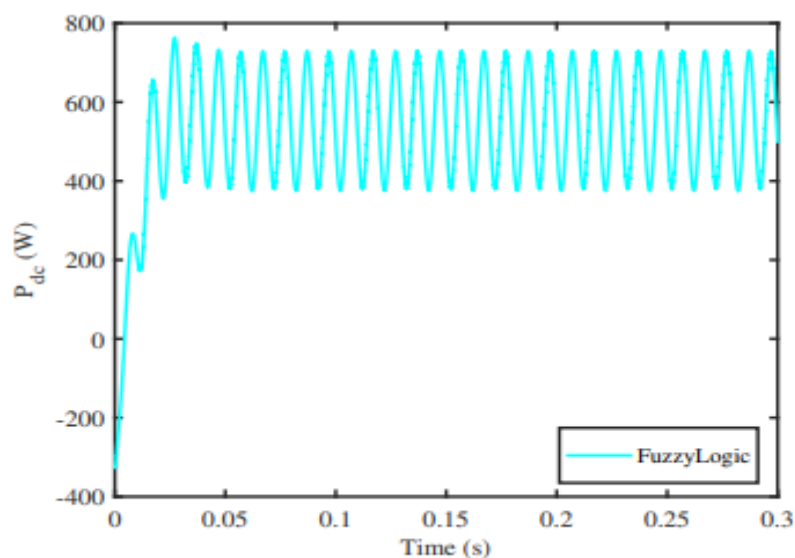


Figure 23: Battery power using fuzzy logic control

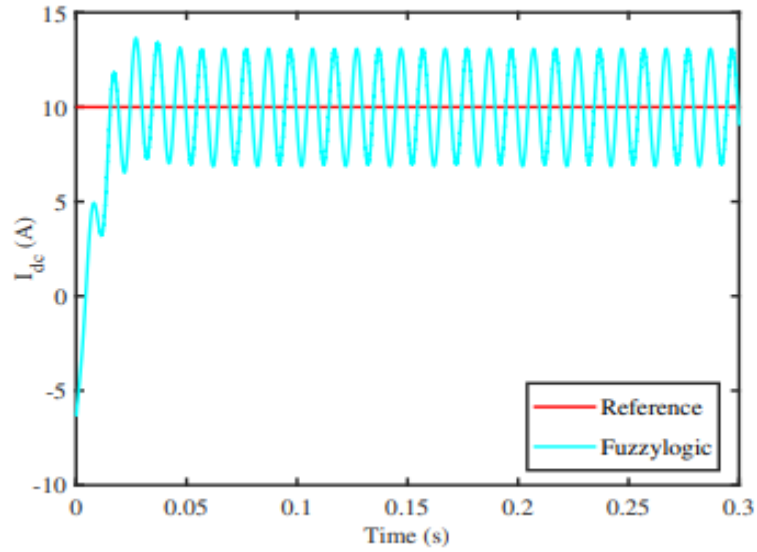


Figure 24: Actual current flowing through the battery for controller

4.3 Comparison of PID with Fuzzy logic controller

When comparing the battery current in both controller scenarios, the current with Fuzzy Logic tracks the reference with faster convergence time than the PID, indicating Fuzzy Logic's superior performance over PID as shown in the zoomed-in portion of Figure 26.

For quick tracking, Fuzzy Logic again outperforms PID in terms of battery voltage and power. Both controllers performed well, however the Fuzzy Logic controller outperformed the others due to its faster convergence time as depicted in Figure 25.

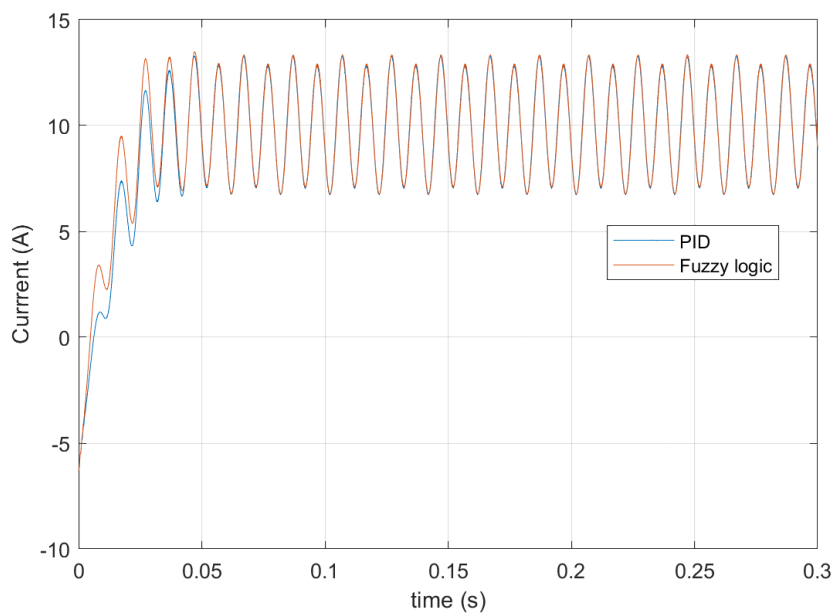


Figure 25: Convergence time of the current

When considering the battery current, FL tracks the reference with faster convergence time and indicates superior performance as shown in the zoomed-in portion of Figure 18.

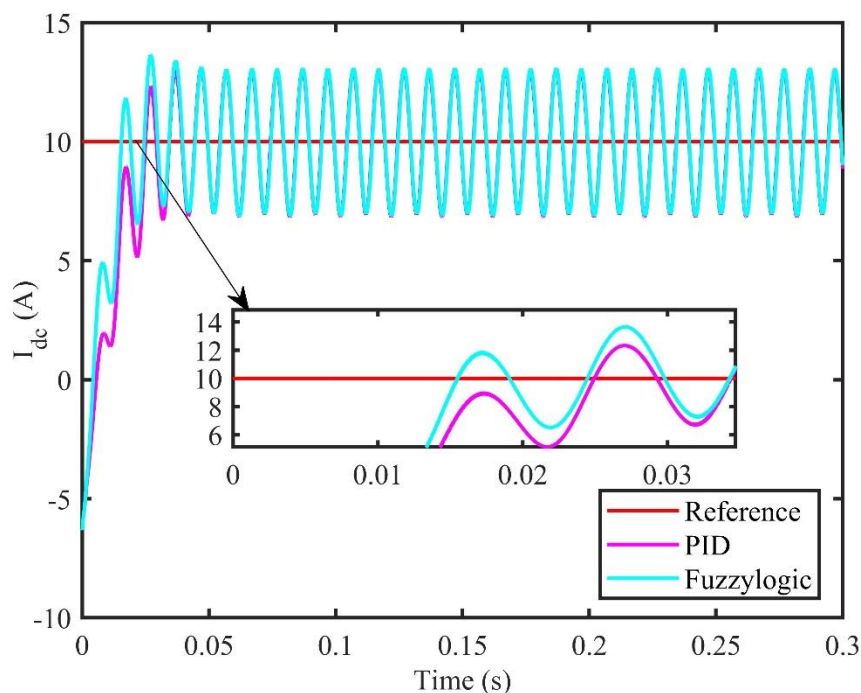


Figure 26: Actual current is flowing through the battery for both controllers

For quick tracking, Fuzzy Logic again outperforms in terms of battery voltage and power. Fuzzy Logic controller outperformed due to its faster convergence time, as depicted in Figure 27, and Figure 28, below:

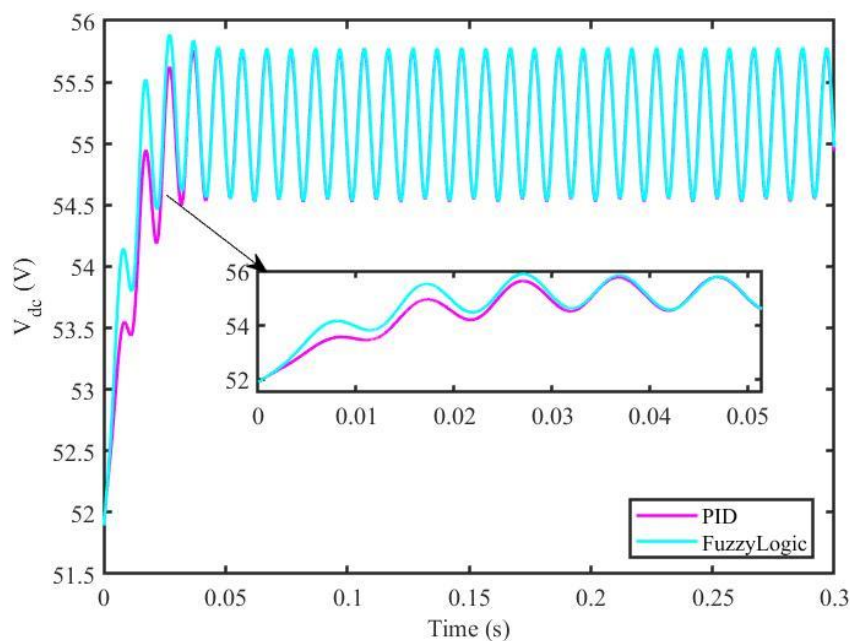


Figure 27: Battery voltage comparison

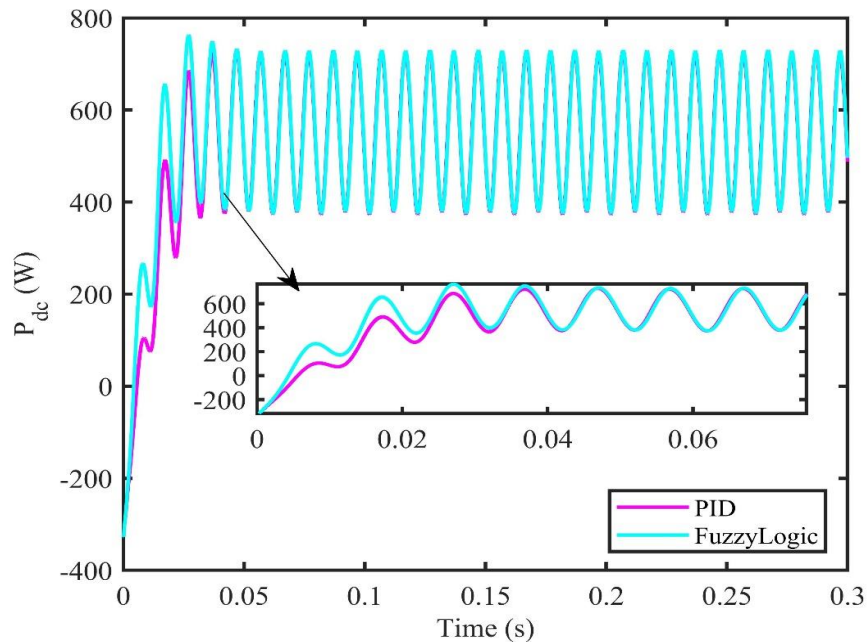


Figure 28: Battery power comparison

4.4 Summary

In this research work the isolated BL Cuk-SEPIC converter's based electric vehicle charger using PID and fuzzy logic controllers' performance was assessed in terms of the systems efficiency, power factor(PF), voltage ripple, and current ripple. MATLAB/Simulink simulations resulted the fuzzy logic controller based system performed better than the PID controller for all measures. More specifically, the fuzzy logic controller provided better control over ripple in voltage(V) and current(I) and showed increased efficiency in a range of circumstances. This shows that the fuzzy logic controller is more resilient and able to deal with erroneous input/output data and uncertainty. Therefore, it is advised that the fuzzy logic controller be used as a more successful control method for isolated bridgeless Cuk-SEPIC converters in chargers for electric vehicles.

CHAPTER 5

CONCLUSION AND FUTURE WORK

5.1 Conclusion

In conclusion, the study showed that, BLS isolated converter charger, fuzzy logic controllers can be evaluated using a simulation for robustness in power quality improvements. The bridgeless configuration of the converter with Cuk and SEPIC is designed to ensure stability. Primary side capacitors have good functionality while strategic use of output inductors results in smooth current flow and effective power factor correction. Proper selection of magnetizing inductance values provides a well-balanced system exhibiting optimal performance with low harmonic distortion. Fuzzy logic control is better than battery current tracking, convergence time, voltage regulation and overall power performance indicating its superior efficiency for proposed charger operation.

5.2 Future Work

Experimental validation and real-world testing have to be done even though it is important to evaluate simulations, they cannot replace real-life tests which are necessary for the BLS Isolated Converter Charger's practical verification. Future studies should include creating and evaluating hardware prototypes that verify the findings from simulation results as well as assess functional metrics such as durability and reliability as well as power quality (PQ) improvement accomplished in everyday life.

Enhanced fuzzy logic algorithms could be used for investigation into the improved fuzzy logic algorithms or hybrid control strategies could be advanced by further research which may also involve other approaches like genetic or neural networks.

References

- [1] J. Larminie and J. Lowry, *Electric vehicle technology explained*. John Wiley & Sons, 2012.
- [2] A. Emadi, M. Ehsani, and J. M. Miller, *Vehicular electric power systems: land, sea, air, and space vehicles*. CRC press, 2003.
- [3] A. Emadi, Y. J. Lee, and K. Rajashekara, "Power electronics and motor drives in electric, hybrid electric, and plug-in hybrid electric vehicles," *IEEE Transactions on industrial electronics*, vol. 55, no. 6, pp. 2237–2245, 2008.
- [4] A. Prudenzi, U. Grasselli, and R. Lamedica, "Iec std. 61000-3-2 harmonic current emission limits in practical systems: need of considering loading level and attenuation effects," in *2001 Power Engineering Society Summer Meeting. Conference Proceedings (Cat. No. 01CH37262)*, vol. 1, pp. 277–282, IEEE, 2001.
- [5] R. Kushwaha, B. Singh, and V. Khadkikar, "An isolated bridgeless cuk–sepic converter-fed electric vehicle charger," *IEEE Transactions on Industry Applications*, vol. 58, no. 2, pp. 2512–2526, 2021.
- [6] L. Petersen and M. Andersen, "Two-stage power factor corrected power supplies: The low component-stress approach," in *APEC. Seventeenth annual IEEE applied power electronics conference and exposition (Cat. No. 02CH37335)*, vol. 2, pp. 1195–1201, IEEE, 2002.
- [7] C. Li, Y. Zhang, Z. Cao, and X. Dewei, "Single-phase single-stage isolated zcs current-fed full-bridge converter for high-power ac/dc applications," *IEEE Transactions on Power Electronics*, vol. 32, no. 9, pp. 6800–6812, 2016.
- [8] F. Musavi, M. Edington, W. Eberle, and W. G. Dunford, "Evaluation and efficiency comparison of front-end ac-dc plug-in hybrid charger topologies," *IEEE Transactions on Smart grid*, vol. 3, no. 1, pp. 413–421, 2011.
- [9] F. Musavi, W. Eberle, and W. G. Dunford, "A high-performance single phase bridgeless interleaved pfc converter for plug-in hybrid electric vehicle battery chargers," *IEEE Transactions on Industry Applications*, vol. 47, no. 4, pp. 1833–1843, 2011.
- [10] M. Pahlevaninezhad, P. Das, J. Drobnik, P. K. Jain, and A. Bakhshai, "A zvs interleaved boost ac/dc converter used in plug-in electric vehicles," *IEEE Transactions on Power Electronics*, vol. 27, no. 8, pp. 3513–3529, 2012.

- [11] G. Li, J. Xia, K. Wang, Y. Deng, X. He, and Y. Wang, "A singlestage interleaved resonant bridgeless boost rectifier with high-frequency isolation," *IEEE Journal of Emerging and Selected Topics in Power Electronics*, vol. 8, no. 2, pp. 1767–1781, 2019.
- [12] H. Wang, S. Dusmez, and A. Khaligh, "Design and analysis of a fullbridge llc-based pev charger optimized for wide battery voltage range," *IEEE Transactions on Vehicular technology*, vol. 63, no. 4, pp. 1603–1613, 2013.
- [13] A. K. Singh, A. K. Mishra, K. K. Gupta, P. Bhatnagar, and T. Kim, "An integrated converter with reduced components for electric vehicles utilizing solar and grid power sources," *IEEE Transactions on Transportation Electrification*, vol. 6, no. 2, pp. 439–452, 2020.
- [14] Y. Jang and M. M. Jovanovi'c, "Bridgeless high-power-factor buck converter," *IEEE Transactions on Power Electronics*, vol. 26, no. 2, pp. 602–611, 2010.
- [15] K. K. M. Siu and C. N. M. Ho, "Manitoba rectifier—bridgeless buck– boost pfc," *IEEE Transactions on Power Electronics*, vol. 35, no. 1, pp. 403–414, 2019.
- [16] B. Singh, S. Singh, A. Chandra, and K. Al-Haddad, "Comprehensive study of single-phase ac-dc power factor corrected converters with highfrequency isolation," *IEEE transactions on Industrial Informatics*, vol. 7,no. 4, pp. 540–556, 2011.
- [17] S. Dian, X. Wen, X. Deng, and S. Zhang, "Digital control of isolated cuk power factor correction converter under wide range of load variation," *IET Power Electronics*, vol. 8, no. 1, pp. 142–150, 2015.
- [18] B. Singh and A. Anand, "Power factor correction in modified sepic fed switched reluctance motor drives," *IEEE Transactions on Industry Applications*, vol. 54, no. 5, pp. 4494–4505, 2018.
- [19] R. Kushwaha and B. Singh, "A unity power factor converter with isolation for electric vehicle battery charger," in *2018 IEEMA Engineer Infinite Conference (eTechNxT)*, pp. 1–6, IEEE, 2018.

- [20] A. Ahmad, M. S. Alam, and R. Chabaan, "A Comprehensive Review of Wireless Charging Technologies for Electric Vehicles," *IEEE Trans. Transp. Electrification*, 2017.
- [21] J. García-Villalobos, I. Zamora, J. I. San Martín, F. J. Asensio, and V. Aperribay, "Plug-in electric vehicles in electric distribution networks: A review of smart charging approaches," *Renewable and Sustainable Energy Reviews*. 2014.
- [22] S. Habib, M. Kamran, and U. Rashid, "Impact analysis of vehicle-to-grid technology and charging strategies of electric vehicles on distribution networks - A review," *J. Power Sources*, vol. 277, pp. 205–214, 2015.
- [23] I. Rahman, P. M. Vasant, B. S. M. Singh, M. Abdullah-Al-Wadud, and N. Adnan, "Review of recent trends in optimization techniques for plug-in hybrid, and electric vehicle charging infrastructures," *Renew. Sustain. Energy Rev.*, vol. 58, pp. 1039–1047, 2016.
- [24] K. M. Tan, V. K. Ramachandramurthy, and J. Y. Yong, "Integration of electric vehicles in smart grid: A review on vehicle to grid technologies and optimization techniques," *Renew. Sustain. Energy Rev.*, vol. 53, pp. 720–732, 2016.
- [25] M. J. Hodgson and K. E. Rosling, "A network location-allocation model trading off flow capturing and p-median objectives," *Ann. Oper. Res.*, 1992. [7] C. Upchurch, M. Kuby, and S. Lim, "A model for location of capacitated alternative-fuel stations," *Geogr. Anal.*, 2009.
- [26] W. Su, H. Eichi, W. Zeng, and M. Y. Chow, "A survey on the electrification of transportation in a smart grid environment," *IEEE Transactions on Industrial Informatics*. 2012.
- [27] C. Hutson, G. K. Venayagamoorthy, and K. A. Corzine, "Intelligent scheduling of hybrid and electric vehicle storage capacity in a parking lot for profit maximization in grid power transactions," 2008 IEEE Energy 2030 Conf. ENERGY 2008, 2008.

- [28] A. Awasthi, D. Chandra, S. Rajasekar, A. K. Singh, A. D. V. Raj, and K. M. Perumal, "Optimal infrastructure planning of electric vehicle charging stations using hybrid optimization algorithm," 2016 Natl. Power Syst. Conf. NPSC 2016, 2017.
- [29] M. R. Mozafar, M. H. Moradi, and M. H. Amini, "A simultaneous approach for optimal allocation of renewable energy sources and electric vehicle charging stations in smart grids based on improved GA-PSO algorithm," *Sustain. Cities Soc.*, vol. 32, pp. 627–637, 2017.
- [30] M. H. Amini, A. Kargarian, and O. Karabasoglu, "ARIMA-based decoupled time series forecasting of electric vehicle charging demand for stochastic power system operation," *Electr. Power Syst. Res.*, vol. 140, pp. 378–390, 2016.
- [31] I. Rahman, P. M. Vasant, B. S. M. Singh, and M. Abdullah-AlWadud, "On the performance of accelerated particle swarm optimization for charging plug-in hybrid electric vehicles," *Alexandria Eng. J.*, vol. 55, no. 1, pp. 419–426, 2016.
- [32] P. M. Vasant, I. Rahman, B. S. M. Singh, and M. Abdullah-AlWadud, "Optimal power allocation scheme for plug-in hybrid electric vehicles using swarm intelligence techniques," *Cogent Eng.*, vol. 3, no. 1, 2016.
- [33] F. Kley, C. Lerch, and D. Dallinger, "New business models for electric cars-A holistic approach," *Energy Policy*, vol. 39, no. 6, pp. 3392–3403, 2011.
- [34] S. Árpád Funke, T. Gnann, and P. Plötz, "Addressing the different needs for charging infrastructure: An analysis of some criteria for charging infrastructure set-up," *Green Energy Technol.*, vol. 203, pp. 73–90, 2015.
- [35] P. Morrissey, P. Weldon, and M. O'Mahony, "Future standard and fast charging infrastructure planning: An analysis of electric vehicle charging behaviour," *Energy Policy*, vol. 89, no. 2016, pp. 257–270, 2016.

- [36] H. Zhang, S. J. Moura, Z. Hu, and Y. Song, "PEV Fast-Charging Station Siting and Sizing on Coupled Transportation and Power Networks," *IEEE Trans. Smart Grid*, 2018.
- [37] W. Yuan, J. Huang, and Y. J. Zhang, "Competitive Charging Station Pricing for Plug-In Electric Vehicles," *IEEE Trans. Smart Grid*, 2017.
- [38] F. He, D. Wu, Y. Yin, and Y. Guan, "Optimal deployment of public charging stations for plug-in hybrid electric vehicles," *Transp. Res. Part B Methodol.*, 2013.
- [39] Z. Liu, F. Wen, and G. Ledwich, "Optimal planning of electricvehicle charging stations in distribution systems," *IEEE Trans. Power Deliv.*, 2013.
- [40] M. Nilsson, "Electric Vehicles: the Phenomenon of Range Anxiety," *ELVIRE Consort.*, pp. 1–16, 2011.
- [41] W. Feng and M. Figliozzi, "An economic and technological analysis of the key factors affecting the competitiveness of electric commercial vehicles: A case study from the USA market," *Transp. Res. Part C Emerg. Technol.*, vol. 26, pp. 135–145, 2013.
- [42] Z. Li and M. Ouyang, "The pricing of charging for electric vehicles in China-Dilemma and solution," *Energy*, vol. 36, no. 9, pp. 5765– 5778, 2011.
- [43] M. K. Hidrue, G. R. Parsons, W. Kempton, and M. P. Gardner, "Willingness to pay for electric vehicles and their attributes," *Resour. Energy Econ.*, vol. 33, no. 3, pp. 686–705, 2011